

Generalized method of image and the tunneling spectroscopy in high- T_c superconductors

Shin-Tza Wu¹ and Chung-Yu Mou^{1,2}

1. Department of Physics, National Tsing Hua University, Hsinchu 30043, Taiwan
 2. National Center for Theoretical Sciences, P.O.Box 2-131, Hsinchu, Taiwan

(Dated: November 2, 2018)

A generalized method of image is developed to investigate the tunneling spectrum from the metal into a class of states, with the tight-binding dispersion fully included. The broken reflection symmetry is shown to be the necessary condition for the appearance of the zero-bias conductance peak (ZBCP). Applying this method to the d -wave superconductor yields results in agreement with experiments regarding the splitting of ZBCPs in magnetic field. Furthermore, a ZBCP is predicted for tunneling into the (110) direction of the d -density wave state, providing a signature to look for in experiments.

PACS numbers: PACS numbers: 74.20.-z, 74.50.+r, 74.80.FP, 74.20.Mn

The current transport through a heterojunction consisting of a normal metal and another different material (X) has been the subject of interest for many years. In this setup, the normal metal with known spectral properties is used as a probe to analyze the electronic states of the material X .¹ Although such measurements have provided useful insights into the bulk spectral properties of X , it has been also realized that the presence of the interface matters. The zero-bias conductance peak (ZBCP) observed in the tunneling spectra when X is a d -wave superconductor (ND junction) in (110) direction² is a well-known example of interface effects. However, the issue of exactly how the tunneling measurements are related to the bulk properties has never been answered satisfactorily. Conventionally, the ND junction is analyzed in the mean-field level, using the Bogoliubov de Gennes (BdG) equations in which continuum and quasi-classical approximations are often invoked. While these approximations are valid for conventional superconductors, they are certainly not justified for high T_c cuprates where proximity to the Mott insulators entails fully consideration of the tight-binding nature. Previously³ this was done by numerically solving the discrete BdG equation for each interface orientation individually without elucidating their relations to the bulk properties. This technical inconvenience makes it difficult to include fluctuations systematically in this approach.

In this work, we shall adopt a different approach based on the non-equilibrium Keldysh-Green's function formalism which enables one to construct systematically higher order corrections from the mean field lattice Green's functions.^{4,5,6} In this approach, because X extends over a semi-infinite space, one shall need the half-space Green's functions. For simple configurations such as the (100) orientation of a d -wave superconductor, it turns out that this half-space Green's functions only differ from the bulk ones by sinusoidal factors. This relation certainly does not hold for other orientations as it predicts no ZBCP in the (110) direction. We shall develop a generalized method of image which enables us to construct the half-space Green's function from the bulk ones. *We empha-*

size the generality of this method and its ability to account for the low energy features in the tunneling spectrum for a whole class of states. As a demonstration, in this article we will focus mostly on the study of ND junctions and only briefly mention the applications to other systems. The effects of interactions and fluctuations will be addressed elsewhere.

Our results indicate broken reflection symmetry is necessary for the emergence of ZBCP. For ND junctions our method can reproduce earlier results on the ZBCP in the continuous wave approximation.^{2,7} In a full tight-binding calculation for (110) and (210) directions, we obtain the doping dependence of the ZBCPs which shows its sensitivity to the Fermi surface topology. In particular, the splitting of the ZBCP in the current-carrying state is also calculated and is shown to be in agreement with experiments. At the end, we analyze the case when X is the d -density wave (DDW) state in (110) direction and the semi-infinite graphene sheet with a zig-zag type interface. The former state was recently proposed as a possible normal state for high T_c cuprates.⁸ Conductance peaks are found for both states.

We start by considering a junction consisting of a 2D normal metal on the left (L) hand side ($-\infty < x \leq -d$, d is the lattice constant of the metal side) and a d -wave superconductor ($0 \leq x < \infty$) on the right (R) hand side (see Fig. 1), governed by the Hamiltonian H_L and H_R respectively. At the mean-field level, we have

$$H_R = - \sum_{\langle ij \rangle, \sigma} t_R c_{i\sigma}^\dagger c_{j\sigma} - \sum_{\langle ij \rangle', \sigma} t'_R c_{i\sigma}^\dagger c_{j\sigma} + \sum_{\langle ij \rangle} \Delta_{ij} (c_{i\uparrow} c_{j\downarrow} - c_{i\downarrow} c_{j\uparrow}) + \text{H.c.}, \quad (1)$$

where $\langle ij \rangle$ denotes the nearest-neighbor (NN) bond, $\langle ij \rangle'$ the next NN bond, and Δ_{ij} possesses the d -wave symmetry. The tunneling Hamiltonian connects the interface points at $x = -d$ and $x = 0$, and is given by $H_T = \sum_y t(|y_L - y_R|)(c_L^\dagger c_R + c_R^\dagger c_L)$, where the summation is over lattice points along the interface, chosen to be in the y direction. We shall assume that both sides are

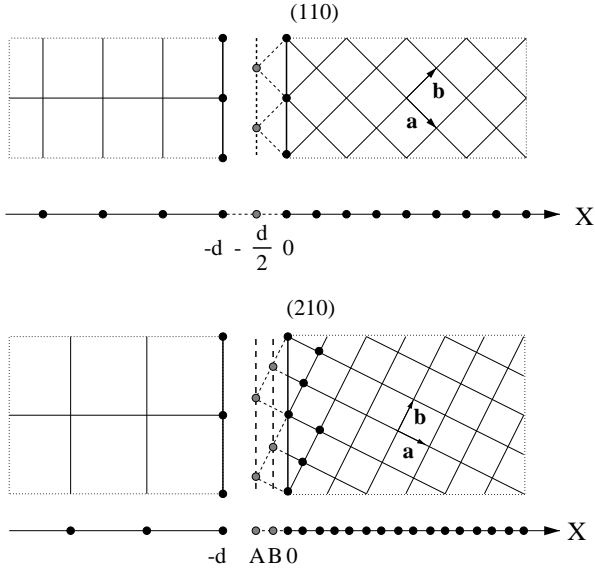


FIG. 1: Schematic plot of the ND junction in (110) and (210) directions. Here two hard walls for the (210) case are at $A = -2d/\sqrt{5}$ and $B = -2d/\sqrt{5}$. The dots on the x axis are the reduced 1D lattice points.

square lattices and characterize the orientation of RHS by the Miller indices $(hk0)$. The total grand Hamiltonian is then given by $K = (H_L - \mu_L N_L) + (H_R - \mu_R N_R) + H_T \equiv K_0 + H_T$. Here μ_L and μ_R are the chemical potentials and their difference $\mu_L - \mu_R$ is fixed to be the voltage drop eV across the junction.

In the non-equilibrium Keldysh-Green's function formalism, H_T is adiabatically turned on.^{4,5} As a result, the bare Green's function is defined only on a half plane. Since the nearest-neighbor bonds to the interface sites are cut, there is effectively a hard wall located at say, for the (110) interface, $x = -d/2$. This hard-wall boundary condition prompts the application of the method of image. However, because lattice points in the half-plane usually do not form a simple Bravais lattice and the d -wave gap changes sign under reflection, the implementation of the conventional method of image appears problematic. To overcome these difficulties, a Fourier transform in the y direction is performed first. Consider the case of (110) orientation, the Hamiltonian with only NN hopping becomes

$$\begin{aligned}
 H_R = & \sum_{i,\sigma,k_y} -2t_R \cos\left(\frac{k_y d}{2}\right) c_{i\sigma}^\dagger(k_y) c_{i+1\sigma}(k_y) \\
 & + \sum_{i,k_y} 2i\Delta_0 \sin\left(\frac{k_y d}{2}\right) [c_{i\uparrow}(k_y) c_{i+1\downarrow}(-k_y) \\
 & \quad + c_{i\downarrow}(-k_y) c_{i+1\uparrow}(k_y)] + \text{H.c.}, \quad (2)
 \end{aligned}$$

where $-\pi/d < k_y \leq \pi/d$ and $2\Delta_0$ is the gap value. The whole problem is now one dimensional, and the hard wall becomes a point. Note that the suppression of the gap near the interface can be taken into account

by adding self-consistent $\delta\Delta_0(i)$ to Eq. (2), and can be treated perturbatively later. In the presence of t'_R , additional terms $\sum_{i,\sigma,k_y} -2t'_R \cos(k_y d) c_{i\sigma}^\dagger(k_y) c_{i\sigma}(k_y) + t'_R c_{i\sigma}^\dagger(k_y) c_{i+2\sigma}(k_y) + \text{H.c.}$ appear. Since at the boundary, both t_R and t'_R are cut and become dangling bonds, one needs to introduce two hard walls at $x = -d/2$ and $x = -d$. For clear presentation, we shall first set $t'_R = 0$. In this case, we are looking for the Green's function, $\bar{G}_0(\omega, k_y, x, x')$ (which is a 2×2 matrix in Nambu's notations), that satisfies the boundary condition $\bar{G}_0 = 0$ at $x = -d/2$. We shall suppress the dependence on ω and k_y . Here since x' is the location of the point source and its image point is at $-d - x'$,⁹ the method of image can be employed by constructing

$$\bar{G}_0(x, x') = G_0(x - x') - G_0(x + d + x') \alpha(x'), \quad (3)$$

where G_0 is the bulk bare Green's function and α is a matrix to be determined. The first term is the direct propagation from x' to x , while the second term will reduce to the propagation from the image point to x in special situations (see below). In fact, since \bar{G}_0 has to vanish at $x = -d/2$, we obtain $\alpha(x') = G_0^{-1}(d/2 + x') G_0(-d/2 - x')$. Therefore, the second term describes the propagation from x' to x via the reflection of the hard wall. The matrix α , apart from fitting the boundary condition, carries the important information about the gap structure along the reflected path from x' to x . Note that in calculating the tunneling current, since H_T only connects points along the interface, only the surface Green's function $\bar{g}_0(\omega, k_y) \equiv \bar{G}_0(x = 0, x' = 0)$ is needed.^{4,10} Writing G_0 in the Fourier k_x space, we find

$$\bar{g}_0(\omega, k_y) \equiv \int_{-2\pi/d}^{2\pi/d} \frac{dk_x}{2\pi} G_0(\omega, k_y, k_x) [1 - \exp(ik_x d) \alpha_0], \quad (4)$$

where the factor $\alpha_0 = G_0^{-1}(d/2) G_0(-d/2)$ is independent of k_x . If the reflection symmetry holds for the state X , such as d -wave superconductors in (100) direction (in this case, $d/2$ is replaced by d), one has $\alpha_0 = 1$ and Eq. (4) reduces to the familiar form⁴ $\bar{g}_0(\omega, k_y) \equiv \int_{-2\pi/d}^{2\pi/d} dk_x / \pi G_0(\omega, k_y, k_x) \sin^2(k_x d/2)$. Therefore, apart from modifications due to the sinusoidal factors, the density of state almost has the same feature as the bulk one. However, for other orientations such as the (110) direction, reflection symmetry with respect to the interface is broken. As a result, α_0 is not the identity matrix and as we shall see, this will give rise to the ZBCP.

The advantage of Eq. (4) is that it is purely based on the bulk Green's functions. The interface orientation is encoded in k_x and k_y . In other words, $G_0(\omega, k_y, k_x)$, which appears in Eq. (4) and α_0 , is simply the usual bulk BCS Green's function but with \mathbf{k} being rotated by 45° . This technical merit is retained for other interface orientations with \mathbf{k} being rotated by the angle in accordance with the interface orientation. More importantly,

this also offers a scheme for studying fluctuations and interactions. Essentially one can take into account these effects through the bulk Green's function G_0 . This will be explained in more detail in a separate publication.

When evaluating $G_0(x-x')$, the dominant contributions come from the poles determined by $(\omega+i\eta)^2 - E_k^2 = 0$, where $E_k = \sqrt{\epsilon_k^2 + \Delta_k^2}$. In the continuum limit, the dispersion becomes $\epsilon_k = \hbar^2(k_x^2 - k_{Fx}^2)/2m$ and $\Delta_k = \Delta_0 \cos 2(\theta - \theta_0)$, where $k_{Fx}^2 = k_F^2 - k_y^2$, $\theta = \sin^{-1}(k_y/k_F)$, and θ_0 is the angle between the crystal a axis and x direction. At the same time, the integration range of k_x is extended to $\pm\infty$. There are four poles located at $\pm k_{\pm}$ with $k_{\pm} \equiv \sqrt{k_{Fx}^2 \pm 2m\sqrt{(\omega+i\eta)^2 - |\Delta_{\pm}|^2}/\hbar^2}$, representing particles and holes along different directions. Here Δ_{\pm} are gaps in directions $\pm\theta$. By contour integration, one obtains $G_0(x-x')$ and thus $\alpha(x')$. After some algebra and assuming that k_F is large,¹¹ indeed Eq.(3) reproduces results obtained in Ref. 7 by direct solving the equations of motion. In our approach, the continuum approximation is not necessary. To investigate any effect that is due to the tight binding nature, the full tight binding dispersion has to be retained. In this case, the integration over k_x can not be extended to $\pm\infty$, and thus poles are in different structure and a substantial difference from the continuum approximation could result.

We now include the hopping t'_R for the (110) direction. The main complication is to add a second hard wall at $x = -d$. This is a simple generalization of the single hard-wall problem. One simply requires \tilde{G}_0 vanish on all these hard walls simultaneously. Therefore, we write

$$\tilde{G}_0(x, x') = G_0(x-x') - G_0(x-x'_1)\alpha_1(x') - G_0(x-x'_2)\alpha_2(x'), \quad (5)$$

where $x'_1 = -x' - d$ and $x'_2 = -x' - 2d$ are images of x' . The boundary conditions at $x = -d$ and $x = -2d$ determines α_1 and α_2 . The surface Green's function thus obtained is the bare one and will get renormalized by H_T , giving rise to four different components in the differential conductance^{4,11}. The strength of H_T , characterized by t , determines the relative weight among each component. In Fig. 2, we show our results for the spectrum of the total differential conductance for various dopings. The parameters adopted are determined self-consistently from the mean-field slave-boson theory for the t - t' - J model.⁴ It is clear that the ZBCPs are the most important features at low energies.² Since the ZBCP arises from the existence of zero-energy states, it must appear as poles at zero energy in the Green's function. For (110) direction without t'_R , this is entirely determined by zeros of the denominator in α :

$$\beta(\omega, k_y) = \det[G_0(d/2)]. \quad (6)$$

In the continuum limit ($d \rightarrow 0$), β can be evaluated analytically: $\beta \approx -[\omega^2/\Delta^2 + (\Delta_+/|\Delta_+| + \Delta_-/|\Delta_-|)^2]$ with $\tilde{\Delta} = |\Delta_+||\Delta_-|/(|\Delta_+| + |\Delta_-|)$. Therefore, poles of \tilde{g}_0 at $\omega = 0$ depends crucially on whether there is a sign

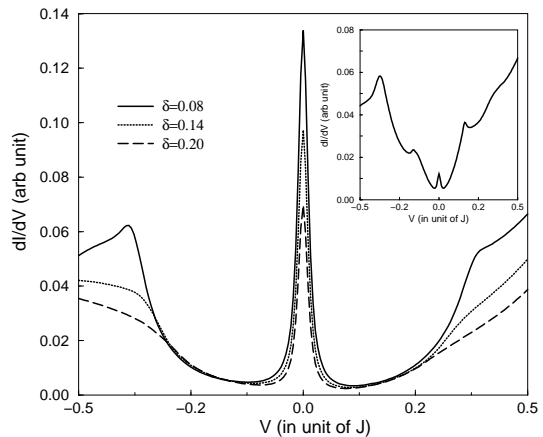


FIG. 2: The total differential conductance of several dopings for (110) interface with $\eta = 0.01$ and $t_L = 1.0$. The weak link is modeled by the interface hopping $t(\omega) = \exp(-\sqrt{(\omega_0 - |\omega|)/\Gamma})$ with $\omega_0 = 11\Delta_0$ and $\Gamma = \Delta_0$. Inset: dI/dV curve for (210) interface with $\delta = 0.08$.

change of the gap on the Fermi surface. This criterion, however, does not hold as one goes to the tight binding limit because pairing no longer only occurs on the Fermi surface. As a result, a numerical computation of β is necessary. Our results indicate that ZBCPs are sensitive to the Fermi surface topology. In fact, for (110) surface, the height of the peak depends on the volume of the Fermi surface. It reaches maximum when $\mu_R = 0$ and decreases when $\mu_R \neq 0$. For other orientations, the ZBCP could even disappear.

For general orientations, there could be more than one hard wall. As a demonstration, we consider the (210) interface. In this case, when $t'_R = 0$, two hard walls are located at $x = -d/\sqrt{5}$ and $-2d/\sqrt{5}$, in analogy to the (110) surface with t'_R . A typical result for small scale of t is shown in the inset of Fig. 2. As t increases, the zero-energy states are able to leak out, and thus the ZBCPs get broadened. Note that lattice points with dangling bonds form a pair-breaking region near the interface, resulting in the peaks around $2\Delta_0$. They are due to quasi-particle bound states with non-zero energy.¹²

The ZBCPs split in the presence of magnetic fields H , essentially due to the Doppler shift caused by the supercurrent near the interface.¹³ In the tight-binding model, Δ_{ij} is shifted to $\Delta_{ij} \exp[i\mathbf{q} \cdot (\mathbf{r}_i + \mathbf{r}_j)]$, where $q = eH\lambda/2\hbar c$ with λ being the penetration depth. By redefining $c_{i\sigma} = c_{i\sigma} \exp(i\mathbf{q} \cdot \mathbf{r}_i)$, the dependence on \mathbf{q} can be absorbed into ϵ_k . Figure 3 shows the field dependence of the splitting for the (110) interface, in agreement to recent experimental data¹⁴. It is seen that for large H , the splitting deviates from linear dependence on H due to the lattice effect in our approach. The inset shows the doping dependence of splitting, reflecting its sensitive dependence on the Fermi surface topology. In fact, in the special case when particle-hole symmetry holds (for ex-

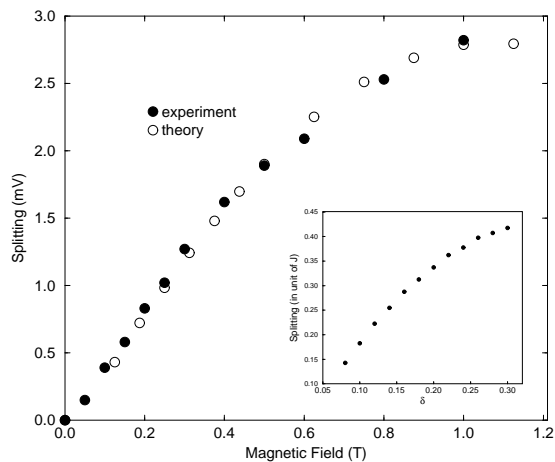


FIG. 3: The field dependence of the splitting for an underdoped case ($\delta = 0.12$). Inset: Doping dependence of the splitting for a fixed magnetic field.

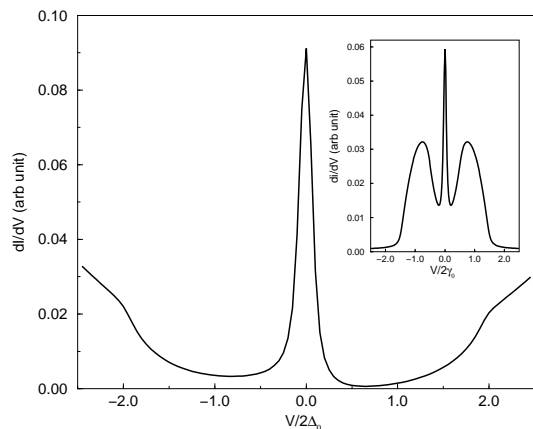


FIG. 4: A typical dI/dV curve for tunneling into the (110) direction of a d -density wave state. Here $\mu_R = 0$ and $\Delta_0 = 0.1$. Inset: A similar plot for tunneling from a wide-band metal into the graphene sheet with zig-zag interface. Here the hopping amplitude $\gamma_0 = 0.1$

ample, $\mu_R = 0$ and $t'_R = 0$), we find that no matter how large H is, the ZBCP does not split at all, in consistent with naive expectations.¹¹

Finally, our approach is easily modified to deal with other states. When X is the DDW, the two-component indices are associated with the two sublattices in this state. The formulation presented for the ND case can then be applied with minor modification.¹¹ At (110) orientation, the DDW state does not possess reflection symmetry; one thus expects ZBCP's in this case. Figure 4 shows a typical result for tunneling into the DDW state in the (110) direction when $\mu_R = 0$. Invariably, the ZBCP is present, consistent with a recent report.¹⁵ For finite μ_R , unlike the d -wave superconductor, one simply adds μ_R to the quasi-particle energy E_k ,⁸ resulting in shifting of the ZBCP to the bias at μ_R . The existence of this conductance peak thus provides a signature of the DDW state. A similar analysis can be done for the semi-infinite graphene sheet. When projected onto 1D lattices, it is then obvious that reflection symmetry is preserved in the case of the armchair interface while not in the zigzag case. This results in for the latter a ZBCP in the dI/dV curve (see the inset of Fig. 4)(Ref. 11) – consistent with previous numerical work.¹⁶ In conclusion, we have developed a versatile formulation for studying the tunneling spectra of junction systems. In particular, it is capable of predicting whether the ZBCP shall arise or not in the conductance curve. The results discussed in this article represent some typical examples; further applications to other systems will be reported elsewhere.

It is our pleasure to thank Professor Sungkit Yip, Professor Hsiu-Hau Lin and Professor T. K. Lee for useful discussions. This research was supported by NSC of Taiwan.

¹ E. L. Wolf, *Principles of Electron Tunneling Spectroscopy* (Oxford University Press, New York, 1985).
² C. R. Hu, *Phys. Rev. Lett.* **72**, 1526 (1994); Y. Tanaka and S. Kashiwaya, *ibid* **74**, 3451 (1995).
³ See for example Y. Tamura *et al.*, *Phys. Rev. B* **60**, 9817(1999).
⁴ C. L. Wu *et al.*, *Phys. Rev. B* **63**, 172503 (2001); X. Z. Yan *et al.*, *ibid* **61**, 14759 (2000).
⁵ C. Caroli *et al.*, *J. Phys. C: Solid St. Phys.* **4**, 916 (1971); J. C. Cuevas *et al.*, *Phys. Rev. B* **54**, 7366 (1996).
⁶ The Green's function approach has also been attempted at quasi-classical level, see for example, T. Luck *et al.*, *Phys. Rev. B* **63**, 064510 (2001).
⁷ M. P. Samanta and S. Datta, *Phys. Rev. B* **57**, 10972

(1998).

⁸ S. Chakravarty *et al.*, *Phys. Rev. B* **63**, 094503 (2001).
⁹ In fact, for 1D, the image point can be chosen arbitrarily without affecting the result.
¹⁰ S. Datta, *Electronic Transport in Mesoscopic Systems* (Cambridge University press, New York) (1995).
¹¹ S. T. Wu and C.-Y. Mou, unpublished.
¹² Y. S. Barush and A. A. Svidzinsky, *Phys. Rev. B* **55**, 15282 (1997).
¹³ M. Fogelstrom *et al.*, *Phys. Rev. Lett.* **79**, 281 (1997).
¹⁴ Y. Dagan and G. Deutscher, *Phys. Rev. Lett.* **87**, 177004 (2001)
¹⁵ C. Honerkamp and M. Sigrist, *J. Phys.-Cond. Matt.* **13** 11669 (2001).

¹⁶ M. Fujita *et al.*, J. Phys. Soc. Jpn. **65**, 1920 (1996).